Int. J. Heat Mass Transfer. Vol. 35, No. 10, pp. 2475–2489, 1992
Printed in Great Britain

0017–9310/92 $5.00 + 0.00

Heat transfer enhancement in coiled tubes by chaotic mixing

NARASIMHA ACHARYA and MIHIR SEN
Department of Aerospace and Mechanical Engineering, University of Notre Dame, Notre Dame, IN 46556, U.S.A.

and

HSUEH-CHIA CHANG
Department of Chemical Engineering, University of Notre Dame, IN 46556, U.S.A.

(*Received* 7 *June* 1991 *and in final form* 11 *October* 1991)

Abstract—The present work examines chaotic mixing as a means of enhancing the in-tube convection heat transfer in helical coils. It is shown that simple modifications of coil geometry can be made to take advantage of this phenomenon. The study focuses on a geometry with the axis of the coil being turned through 90° in a periodic manner, and comparisons are made with a coil without this change in axis. Particle paths are calculated using the classical perturbation solution of Dean for the secondary flow. Chaotic mixing is confirmed by a positive Lyapunov exponent. The temperature field is calculated numerically showing that chaotic mixing is responsible for considerable flattening of the temperature profile and an increase in convective heat transfer. Experiments are conducted with water on two coiled tube geometries over a Reynolds number range of 3000–10 000. The coils are identical in every respect except that one is conventional with constant axis, while the other is with alternating axis. The latter shows a 6–8% higher in-tube heat transfer coefficient due to chaotic mixing, with a corresponding pressure drop increase of 1.5–2.5%.

INTRODUCTION

ENHANCEMENT of convection has been a practical goal of heat transfer science for a long time (see, for example, a review by Zukauskas [1]). Passive techniques that are used can be roughly classified into increased effective heat transfer area and increased mixing methods. External and internal fins fall into the former category, while the latter includes increase of turbulence intensity and unsteady flow through inserts of various kinds, regular mixing in recirculation zones and resonant enhancement of flow instabilities. Some devices, of course, do both.

It is much more difficult to achieve enhancement in cases in which it is not possible to achieve turbulent flow or instability. Laminar flow, in general, gives much poorer rates of heat transfer compared to turbulent or unsteady flow. Consider, for instance, the transport of heat from the fluid to the walls in the in-tube side of a heat exchanger tube. If the steady streamlines are parallel to the walls of the tube, heat transport in a transverse direction is due only to conduction, a relatively slow molecular effect. This process can be enhanced by fluid exchange or mixing between the interior and the region near the walls, increasing thus the advective component of the heat transfer. In a turbulent or unstable flow, on the other hand, such mixing is normally present due to transverse fluctuations in the fluid velocity.

It must be remembered that mixing, be it laminar or turbulent, also leads to momentum transfer in a direction transverse to the flow. Consequently the wall shear stresses and pressure drops are higher, resulting ultimately in larger pumping costs. The pressure drop increase can be quite significant for augmentation procedures such as inserts and internal grooves since they introduce an additional no-slip surface or roughness. It is advantageous then to consider devices which do not involve inserts nor affect the smoothness of the inner wall, but provide enhancement in the degree of fluid mixing.

Mixing by secondary flow in a plane normal to the principal flow direction is commonly used for heat transfer enhancement. Such is the case with vortices, recirculation regions and natural convective cells. The flow in a coiled tube, to take a specific example, is very effective from the point of view of in-tube convection because of secondary motion in the transverse plane; it is known to provide much higher heat transfer rates compared to straight tubes. Comparing the characteristics of a coiled tube with a straight one, it is found that the increase in the Nusselt number is typically much more than the increase in the pressure drop. For this reason it is useful in practical applications, and much theoretical, numerical and experimental work has been done on this geometry (refs. [2–7] among others). Shah and Joshi [8] provide a recent review of the subject.

NOMENCLATURE

A	heat transfer area
A_{cs}	cross-sectional area of tube
a	tube radius
c	specific heat of water
d_n	distance of separation of two particles
De	Dean number $= Re\sqrt{a/R}$
h	convection heat transfer coefficient
h_f	head loss corresponding to pressure drop in coil
k	thermal conductivity
l	circumferential length of single coil
L	total length of coiled tubing
$\dot{m}$	mass flow rate of water in coil
Nu	Nusselt number
Pe	Peclet number
Pr	Prandtl number $= \nu/\alpha$
Q	heat flow rate
R	coil radius
r	radial coordinate
Re	Reynolds number $= Wa/\nu$
t	time
T	fluid temperature
T_{bulk}	fluid bulk temperature
T_{bath}	bath temperature
T_{coil}	coil temperature
T_{in}	temperature of water coming into coil
T_{out}	temperature of water going out of coil
T_w	constant wall temperature
ΔT	$= T_{in} - T_{out}$
ΔT_{lmtd}	logarithmic mean temperature difference
U	overall heat transfer coefficient
u	radial velocity component
v	angular velocity component
w	axial velocity component
W	tube centerline axial velocity
$\bar{W}$	average velocity
z	axial coordinate
z_s	length after which coil switches axis.

Greek symbols

α	thermal diffusivity
δ	radius ratio $= a/R$
θ	angular coordinate
λ	largest Lyapunov exponent
λ_n	exponent of nth map
ν	kinematic viscosity
ψ	coil switching angle.

Subscripts and superscripts

*	dimensional quantity
AA	alternating axis coil
CA	constant axis coil
i	inner
o	outer.

Chaotic mixing

Chaotic advection is a phenomenon which has been studied theoretically and experimentally in recent years [9–13]. It has been shown that if a planar flow within a closed domain is subjected to suitable temporally periodic perturbations at the boundary, the particle paths can be chaotic. The dynamical system for the evolution of particle position is formally Hamiltonian, where the stream function is the Hamiltonian and the phase space is the physical space of the flow. There are some well-known ideas regarding the appearance of chaos in such systems which can be applied. It is found that chaotic mixing is essentially due to the break-up of homoclinic loops into tangles, the intersections of the stable and unstable manifolds giving rise to chaotic behavior [14]. A set of particles can thus be spatially mixed as it is advected by this time-periodic flow field. This concept can be further extended to steady axial flow in ducts with secondary flow in a transverse direction if the duct is geometrically perturbed in the downstream direction. In this manner chaotic mixing becomes much more useful from a practical point of view since many industrial devices involve flow in ducts. Time-periodic perturbations at a boundary which are both difficult and expensive to implement are not necessary.

Various investigators have proposed that this chaotic mixing phenomenon can be exploited to promote mixing and mass transfer in devices [15]. But, mixing is also very effective in enhancing convective heat transfer; thus chaotic mixing could also be used for heat transfer devices. The purpose of this work is to analyze the feasibility of using chaotic mixing as a means of enhancing the in-tube convective heat transfer coefficient in a coiled tube.

One must be careful to distinguish between chaotic and regular mixing. The latter occurs due to secondary motion in a helically coiled tube with laminar, steady flow where it improves the heat transfer substantially. However, the 'streamlines' of the two secondary vortices that are produced in a transverse plane are closed curves, and the fluid particles moving along them do not mix with each other. In fact, the fluid near the core of the vortices does not mix at all. It is possible to perturb this secondary flow by periodic changes in coiling which will generate chaotic particle pathlines and greater mixing. This perturbation can be produced in a relatively simple manner by changing the axis of the coil with spatial periodicity. The hydrodynamics of chaotic particle paths thus produced has been discussed by Lee *et al.* [16], Jones *et al.* [17] and Le Guer and Peerhossaini [18]. The last-named

authors have also spoken about the idea of a heat exchanger based on this concept [19]. Saxena and Nigam [20] have also proposed a mixing device using helical coils but without reference to chaotic transport. The objective of the present work is to point out that it is possible to increase the heat transfer by suitably designing the coils to alter the secondary flow pattern and induce chaotic mixing. We shall compare two different coils: the first is a conventional helical coil with a fixed axis (hereinafter referred to as the constant axis coil, CA) which produces regular mixing, while the other is a new configuration in which there is a periodic change in loop axis (called the alternating axis coil, AA). We shall show by numerical simulations using an analytically obtained flow field and by laboratory experiments that the AA configuration achieves a higher rate of heat transfer compared to a coil with regular mixing.

THEORY

Detailed flow computations in coiled tubes have been carried out by various authors (see ref. [21] for a review by Berger *et al.*). Since our purpose is simply to demonstrate the feasibility of heat transfer enhancement by chaotic mixing and the physical principles involved, we have used the analytical flow field obtained by Dean [22, 23] which has the essential features we need, i.e. the secondary vortices, and which produces the desired chaotic mixing. The energy equation, though linear, is then numerically solved using this flow field to give the temperature distributions and heat transfer characteristics.

Flow computation

Figure 1 shows the alternating axis geometry selected for analysis. Each successive loop of the coil lies on a different plane, P or P' which are mutually perpendicular, so that after completing each loop the axis of curvature changes by 90°. The computations are made under the following assumptions. The flow field is analytically given by the lowest order perturbation solution of Dean [22], which is, of course, strictly valid only for low Dean numbers. It is also assumed that the new flow field is established immediately after the change in coil axis, amounting to a zero entrance length and a low Reynolds number assumption.

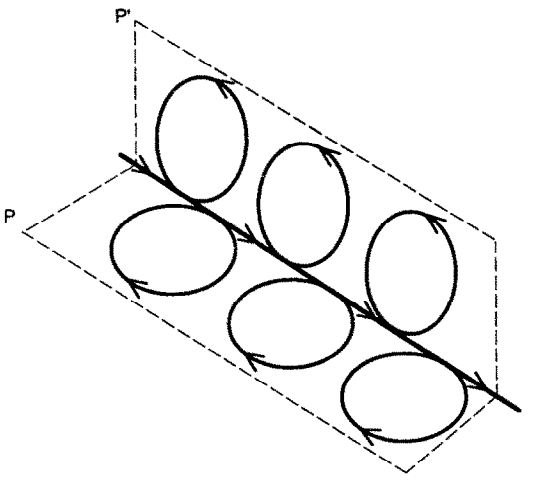

FIG. 1. Geometry of alternating axis coil for chaotic mixing. Arrows indicate flow direction.

The geometry considered is a loosely coiled tube of circular cross-section. A polar coordinate system (r^*, θ, z^*) is employed with r^*, θ and z^* representing the radial, angular and axial coordinates respectively. The tube radius is a, and the coil radius is R. The length or circumference of a single coil is then $l = 2\pi R$. The tube switches its axis after a distance z_s^* which will be indicated as necessary.

The lowest order velocity field is nondimensionally given by [22]

$$u = Re\delta\, f(r, \theta) \tag{1a}$$

$$v = Re\delta\, g(r, \theta) \tag{1b}$$

$$w = 1 - r^2 \tag{1c}$$

where

$$f(r, \theta) = \frac{\sin\theta}{288}(1-r^2)^2(4-r^2) \tag{2a}$$

$$g(r, \theta) = \frac{\cos\theta}{288}(1-r^2)(4-23r^2+7r^4). \tag{2b}$$

The radial coordinate r is nondimensionalized with a, and the velocities with the centerline flow velocity W; (u, v, w) are the nondimensional components of the velocity, Re is the Reynolds number of the flow, and $\delta = a/R$ is the radius ratio. The secondary motion (u, v) in a transverse section generates a pair of Dean vortices. The axial motion w is superposed on this.

The velocity field can be integrated to produce pathlines for any given initial set of fluid particles. Results from the two different coils can be compared by computing the spread of a set of particles simulating the spread of a blob of dye. The switching length z_s for the alternating axis coil is taken to be unity. A set of 400 fluid particles is initially located within the small darkened square shown in Fig. 2(a). For a constant axis coil with regular mixing these particles come out at the positions shown in Fig. 2(b) after an axial distance of $19z_s$. If, on the other hand, the alternating axis coil is used, the same set of initial particles can be seen to mix much more thoroughly over the cross-section of the tube. The locations of the particles at an axial distance of $3z_s$ and $6z_s$ are shown in Figs. 2(c) and (d). In Fig. 2(d), after only five changes in the axis, good mixing appears to have been achieved.

Lyapunov exponents

The Lyapunov exponents, which represent the long-time mean exponential growth rates of neighboring

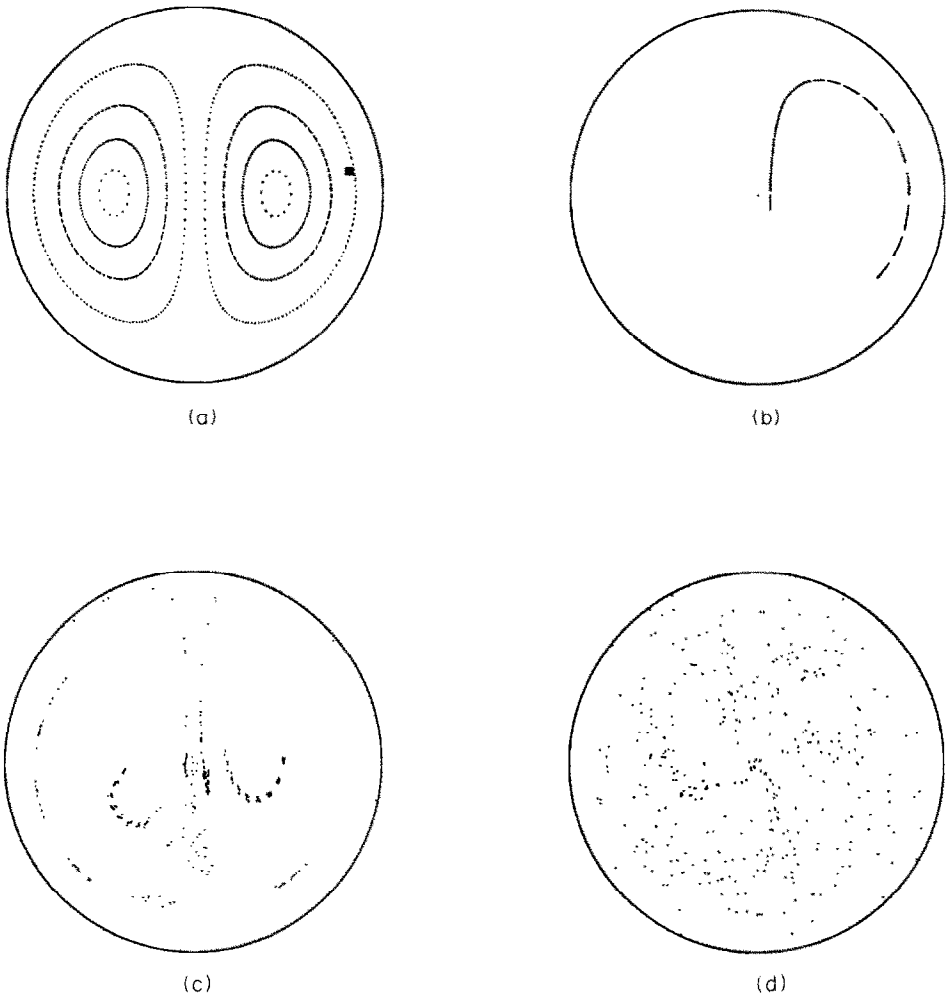

FIG. 2. (a) Secondary flow field at a cross-section with 400 initial particles shown. (b) Final positions of particles, CA coil, axial distance = $19z_s$. (c) Particle positions, AA coil, axial distance = $3z_s$, $\phi = 90°$. (d) Particle positions, AA coil, axial distance = $6z_s$, $\phi = 90°$.

trajectories in phase space, are used to identify the presence of chaos in particle pathlines. We estimate only the largest exponent, which can be obtained from time series measurements of a suitable dynamical variable [24]. A positive value of largest exponent indicates that the system is chaotic.

The secondary motion of the particles obeys a Hamiltonian system and the sum of the Lyapunov exponents is zero. Since Fig. 2(d) shows that there are no 'islands' in the flow domain where chaotic mixing is absent, their trajectories fill up the whole space. Long-time averages starting from any location would then be expected to yield information which is relatively independent of the initial position chosen.

Since particle trajectories can be numerically calculated from the velocity field, we can reduce the flow to a mapping over each period of the coil; every particle at the inlet of a periodic section has its image at the outlet. This mapping is taken over axial intervals of length $2z_s$, which corresponds to a switching length of $1.5l$. The trajectory starting from any initial position is integrated by a fourth order Runge–Kutta scheme, with an axial step size of 0.0025 up to the image plane. Thus there is a sequence of such mappings throughout the length of the coil.

Let us consider the nth mapping which takes two particles separated by a distance of d_n to a separation of d_{n+1}. An exponent λ_n can then be defined as

$$\lambda_n = \frac{1}{n}\sum_{i=1}^{n} \ln\left(\frac{d_{i+1}}{d_i}\right). \tag{3}$$

As $n \to \infty$, $\lambda_n \to \lambda$, the largest Lyapunov exponent for this mapping. For each spatial period of a coil, λ_n is determined. The numerical procedure is continued successively until there is convergence in λ_n.

For the alternating axis case, the exponent value approaches 1.52, varying only slightly with the initial location chosen. A positive Lyapunov exponent confirms that the trajectories are indeed chaotic for this case, and its magnitude is related to the degree of chaotic mixing present in the system. The largest

Lyapunov exponent in case of the constant axis coil lies between -0.005 and 0.005 for different initial locations; it is close to zero indicating the absence of chaos, the slight deviation from zero being due to numerical error.

Heat transfer analysis

Convective heat transfer from the fluid to the walls is due to the combined effect of thermal conduction and advection. Chaotic mixing is most effective in cases where conduction is weak compared to advection. To visualize the influence of coil switch on the temperature profile, consider first the limit of zero conduction, or equivalently, an infinite fluid Prandtl number. Thus the temperature of a fluid particle remains constant as it moves in the flow. By computing the particle paths backwards in the direction of negative time, we can find the positions of the particles at the inlet section which finally end up along a given diameter at the outlet. The temperature profile along the diameter at $\theta = 0$ at the outlet section is plotted in Fig. 3 for an assumed parabolic inlet temperature profile, $T(r) = 1 - r^2$ for both coils. The length of the coil is $10l$, and the switching length is $0.5l$. It is seen that at the outlet, the profile in the case of the alternating axis coil shows a considerably mixed state. It can almost be compared to the instantaneous temperature profile for a turbulent flow. On the other hand, the temperature profile for the constant axis case is regular showing considerably less mixing.

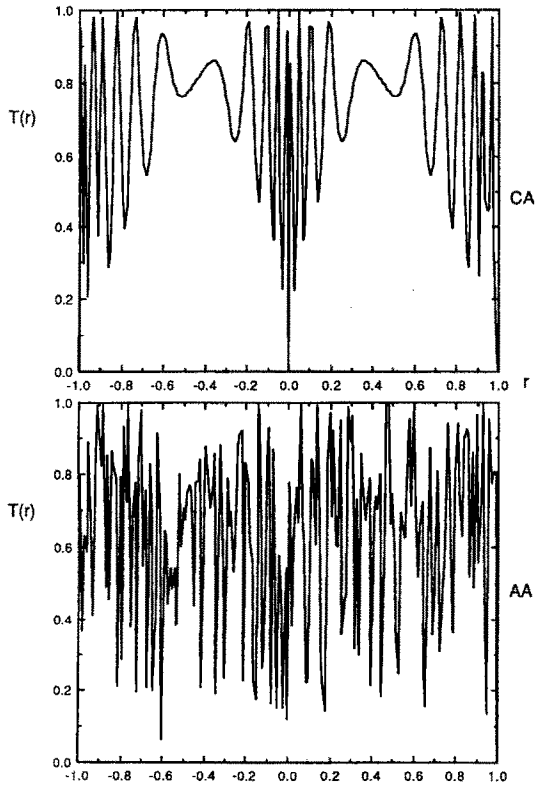

FIG. 3. Temperature profile for infinite Pr, $\phi = 90°$.

For fluids with finite Prandtl number, there will be some thermal diffusion, the effect of which will be to smooth out the temperature profiles. However, to take this into account, it is necessary to solve the energy equation for the temperature field. This will be done numerically using the flow field described by equation (1).

The energy equation is

$$\nabla \cdot (\mathbf{u}^* T^*) = \alpha \nabla^2 T^* \tag{4}$$

where $\mathbf{u}^*$ is the velocity vector, T^* is the temperature, and α is the thermal diffusivity. Neglecting axial conduction and assuming small radius of curvature, we get

$$u^* \frac{\partial T^*}{\partial r^*} + \frac{v^*}{r^*} \frac{\partial T^*}{\partial \theta} + w^* \frac{\partial T^*}{\partial z^{**}} = \alpha \left(\frac{\partial^2 T^*}{\partial r^{*2}} + \frac{1}{r^*} \frac{\partial T^*}{\partial r^*} + \frac{1}{r^{*2}} \frac{\partial^2 T^*}{\partial \theta^2} \right). \tag{5}$$

The boundary conditions are

$$T^* = T_w \quad \text{at } r^* = a \tag{6a}$$

$$T^* = T_{in} \quad \text{at } z^* = 0, \tag{6b}$$

where T_w is the constant wall temperature, and T_{in} is a constant value at the inlet section. We take $T_w \neq T_{in}$.

Nondimensionalizing the axial distance with the coil radius R, and the temperature as

$$T = \frac{T_w - T^*}{T_w - T_{in}},$$

the dimensionless form of the equation is obtained as

$$De^2 Pr \left(f \frac{\partial T}{\partial r} + \frac{g}{r} \frac{\partial T}{\partial \theta} \right) + \delta RePr\, w \frac{\partial T}{\partial z} = \left(\frac{\partial^2 T}{\partial r^2} + \frac{1}{r} \frac{\partial T}{\partial r} + \frac{1}{r^2} \frac{\partial^2 T}{\partial \theta^2} \right) \tag{7}$$

where $De = Re\sqrt{\delta}$ is the Dean number, and Pr is the fluid Prandtl number. This is also the form used by Janssen and Hoogendoorn [25] who performed a similar analysis for coils with constant axis of curvature. The functions $f(r, \theta)$ and $g(r, \theta)$, and the velocity $w(r)$ are given in equations (1) and (2).

The two terms on the LHS of equation (7) represent the effect of heat advection due to secondary flow and principal flow, respectively, while the term on the RHS is the thermal diffusion. The principal flow in the z-direction and the secondary flow in the transverse plane are of the order δPe and $\delta RePe$, where Pe is the Peclet number $= RePr$. As Re goes up, the secondary flow increases in relative strength. As the flow approaches its fully developed nature with a constant wall temperature, the nondimensional bulk temperature approaches a constant value. The secondary flow is then responsible for the advection of heat between the fluid and the walls. This advective term increases with $\delta RePe$, indicating that the best advantage is

obtained with tight coiling, high Reynolds numbers, and large Prandtl number fluids. To take extreme examples, as $\delta \to 0$, the tube becomes straight and secondary flow disappears; as $Re \to 0$, the secondary flow also vanishes; as $Pe \to 0$, the fluid becomes one of high thermal diffusivity in which conduction carries all the heat, and advection is negligible; as $Pe \to \infty$, the material derivative of the temperature $DT/Dt = 0$ so that the temperature does not change on following a fluid particle. In general these remarks are valid for regular mixing as well as chaotic mixing.

The nondimensional form of the boundary conditions (6) is

$$T = 0 \quad \text{at } r = 1 \tag{8a}$$

$$T = 1 \quad \text{at } z = 0. \tag{8b}$$

Numerical procedure

We analyze convective heat transfer in two coils, one with constant axis of coiling and the other with alternating axis. The alternating axis coil has a singly periodic alteration in coil axis; the axis is switched first in a clockwise direction through an angle ϕ, and then back in the counterclockwise direction through the same angle. This switching is repeated as many times as necessary to get convergence in the numerical values. The switching angle ϕ and the switching length z_s are the main geometrical parameters. In the numerical results shown here, $z_s = 10$, corresponding to $1.6l$.

The energy equation is solved by finite differences. Since the equation is parabolic in z, a marching technique using the ADI method is used. The axial derivative is approximated by backward differencing and central differencing is used for the other spatial derivatives. Grid-refinement studies showed that the solution becomes mesh-independent beyond a grid density consisting of 25 divisions in the radial and 48 in the circumferential direction respectively. Accordingly, these values were chosen for all runs.

The Nusselt number is calculated from the expression

$$Nu_z = \frac{2}{T_{\text{bulk}}} \left\langle \left(\frac{\partial T}{\partial r} \right)_{r=1} \right\rangle \tag{9}$$

where T_{bulk} is the fluid bulk temperature, and $\langle\ \rangle$ indicates averaging over the circumferential direction at a particular axial location. This averaging is necessary to take care of the angular variation of the temperature field. This variation arises because the flow is preferentially in the outward direction in the plane of curvature, the temperature field thus developing spatial inhomogeneity. The local Nusselt number is seen to undergo small oscillations in z in the initial development stage but soon settles down to a monotonically varying behavior asymptoting to a fully developed value. Oscillations in Nusselt number for developing temperature profiles have also been reported by several earlier workers [25, 26]. For the alternating axis case, however, the periodic spatial change in the coil axis acts as the mechanism forcing an oscillation. We define, therefore, another average

$$Nu = \langle\langle Nu_z \rangle\rangle \tag{10}$$

where $\langle\langle\ \rangle\rangle$ represents an average over the circumferential direction and also over a length of z_s in the z-direction. The Nusselt number is considered to be fully developed when it varies less than 0.2% in the z-direction.

Comparison tests between the constant and alternating axis coils focused on three system parameters: the Reynolds number, the Prandtl number and the switching angle ϕ. The radius ratio δ is kept constant at 0.1 for all runs. It may be recalled that the use of Dean's solution for the flow field renders the solution valid for small Dean numbers only, i.e. up to about $De = 18$. Consequently, the parameter De^2Pr can be increased only by increasing the Prandtl number of the working fluid. In addition, in order to keep the z axis scaling the same for all parameter ranges studied, so that coil switching may be affected at the same dimensional axial distance z_s^*, it is felt appropriate not to absorb the parameter $\delta RePr$ into the z coordinate. For both these reasons, the Reynolds and Prandtl numbers are kept as separate parameters.

A comment must be made about the pressure drop in the coil. Since the axial flow to lowest order is unaffected in Dean's perturbation solution, the pressure drop computed under this approximation is the same for both the constant axis and the alternating axis coils. It is in fact the same as that for a straight tube. The increase in power required to pump fluid through a coil is thus of lower magnitude than the gain in the heat transfer.

Numerical results

Figure 4 shows the results of the numerical computations expressed in the form of ratios of fully developed Nusselt numbers. Three different cases are compared: the straight pipe (STR), the constant axis coil (CA), and the coil with alternating axis (AA). The corresponding ratios are indicated by the symbols AA/STR, CA/STR, and AA/CA on the graphs.

It is seen that with an increase in the switching angle from zero to 45°, there occurs a significant increase in the heat transfer. For subsequent increase in the switching angle, there is little change in the overall Nusselt number. What the switching action accomplishes is a mixing of particle trajectories so that the resulting temperature profile is flatter than that in a constant axis coil. It can also be seen that the variation in the Nusselt number enhancement is not exactly symmetric about 90°.

The influence of the Reynolds number on the enhancement is of particular interest as one can relate it qualitatively to the experimental results. An increase in Reynolds number increases the strength of the secondary flow vortices and this in turn leads to better mixing within the loops. Consequently, transverse mixing across the central barrier is improved

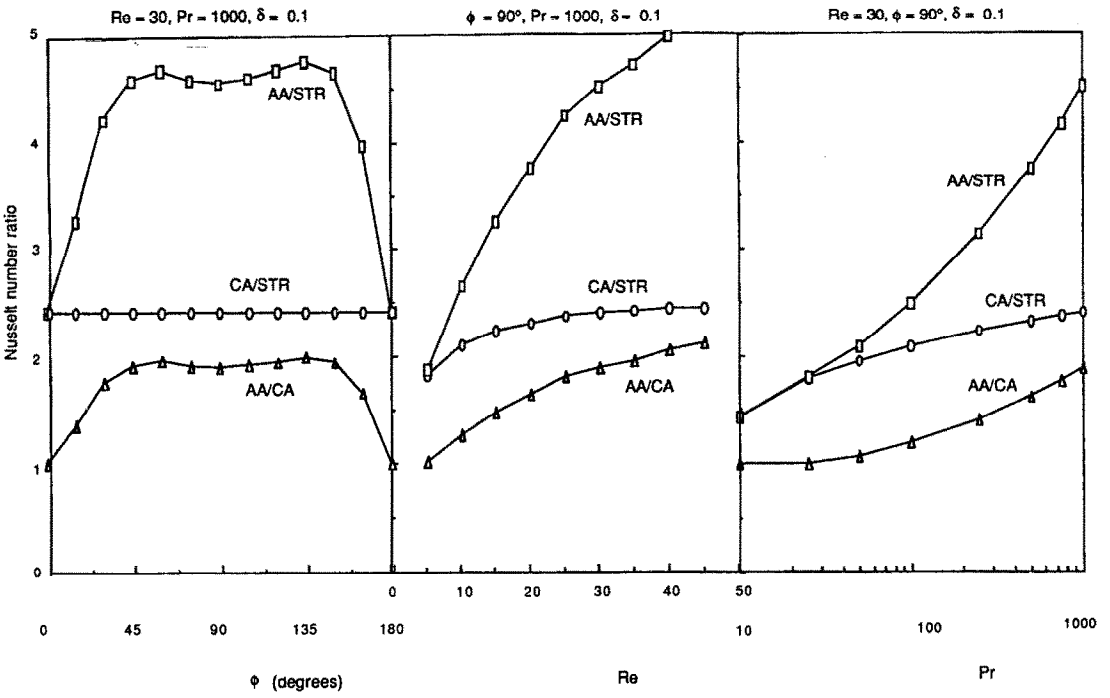

FIG. 4. Nusselt number ratios between straight pipe (STR), constant axis coil (CA), and alternating axis coil (AA). Variation with switching angle ϕ, Reynolds number Re, Prandtl number Pr.

with switching and the enhancement obtained is higher for a larger Reynolds number. This trend will also be observed in experiments to be discussed in a later section.

The Prandtl number is also seen to have an effect similar to the Reynolds number. The significance of this is the fact that the enhanced mixing occurring in the case of the alternating axis coil is a result of convective motion which is strong compared to thermal diffusion for high Prandtl number fluids. For low Prandtl number fluids, diffusion tends to smear out the temperature profile and reduces the effective contribution of the convective transfer. At low Prandtl numbers there is little difference in the heat transfer between the two coils.

Figure 5 shows the temperature profiles at $\theta = 0$ and 90° diameters for two different Prandtl numbers. The temperature profiles display a typical double hump in the transverse plane and perpendicular to the plane of curvature, corresponding to the pair of vortices in the flow. At large Prandtl numbers, the temperature near the wall and tube center drop appreciably due to convective action while the region within the cores of the vortices is practically at the initial temperature. The symmetry in the temperature profile is lost in case of the alternating axis coil due to periodic mixing in the zones adjacent to the plane of axis switching. The flow retains its global character of a double hump since in the regions between the mixing zones, it is still governed by Dean's equations. For the alternating axis coil, the mixing action leads to a chaotic exchange of the cold and hot fluid particles causing the hump to get lower and smeared out. The result is that the temperature profile becomes flatter with a steeper wall temperature gradient accompanied by a smaller bulk temperature. This increases the Nusselt number for the alternating axis coil.

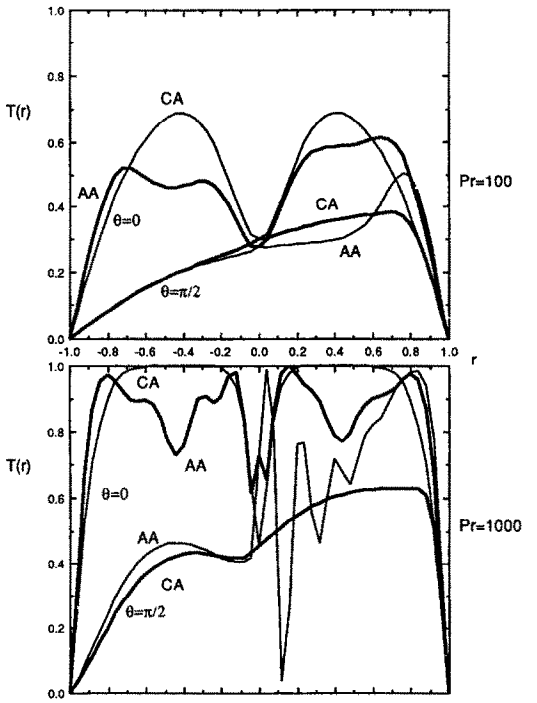

FIG. 5. Temperature profile at $\theta = 0$ and 90° for $Pr = 100$ and 1000. $Re = 30$, $\delta = 0.1$, $\phi = 90°$.

EXPERIMENTS

Comparative experiments on the constant axis and alternating axis coils were carried out in order to obtain a measure of their relative performance in terms of heat transfer and pressure drop. Since the coils were tested over a range of Reynolds numbers, it was felt that the most appropriate comparison should be based on the inner heat transfer coefficient as well as the pressure drop in this range.

The mechanism responsible for the chaotic pathlines is the periodic switching of coil axis in the downstream direction. Thus the effect of chaotic mixing in the alternating axis coil is manifested in the section of the coil immediately downstream of the locations of axis switching. For the rest of the coil, the particle paths and mixing are similar to that in the constant axis coil. Consequently, it would appear that in order to observe a noticeable effect of chaotic mixing, the device should have a large number of axis switches per unit length. But, on the other hand, there is a limitation on the frequency at which this can be done. After a switch of coil axis, the flow field needs a certain transition length before it attains the 'developed' form of Dean vortices and adjusts itself to the new curvature. Chaotic mixing is likely to be most effective when the flow near the end of its transition length is subjected to a switch in coil axis. If the axis is switched much more frequently than this, the effect of chaotic mixing diminishes, an effect that has been observed in our numerical simulations. This points to an optimum switching length for maximum heat transfer enhancement. However, no optimization was attempted because of the inapplicability of the present numerical analysis to experimental conditions.

Experimental set-up

In order to reduce the flow instabilities and fluctuations to a minimum, an open-loop gravity driven flow system was used. For ease of handling, water was used both inside and outside the coils. The overall schematic of the set-up is shown in Fig. 6. Cold water was pumped into a 10 l overhead Nalgene tank (A) at a height of 4 m above the floor level. This tank was inside an overflow chamber B so as to provide a constant head. Water flowed from this tank by gravity through 15.9 mm diameter copper tubing to the test section in bath C, and then to a drain tank which also served as a weigh station. The flow control valves were positioned at a distance of approximately 30 diameters downstream of the test section to minimize flow disturbances upstream.

The test section consisted of three parts, a preconditioner and a post-conditioner coil before and after the coil being tested. The purpose of the preconditioner, 20 diameters long, was to produce an entrance section in which a secondary motion would be set up before the fluid reached the test section. Another objective was to provide enough mixing for the measured temperature to be interpreted as a bulk temperature. The post-conditioner of 15 diameters length reduced the effect of the exit conditions on the test coils, as well as providing once again enough mixing for the temperature measurement. To reduce heat transfer from the conditioner coils to the hot bath, air-filled Plexiglas enclosures were provided around them. These enclosures were fabricated from 6.4-mm thick Plexiglas sheets cut to required size and cemented together with acrylic weld-on liquid.

Considerable effort went into the design and construction of the two coils, identical in every way but their coiling geometry. This was achieved by making the coils out of a number of identical 180° return bends of copper with in-tube and mean coil radii of 10.9 mm and 50.8 mm respectively which were available. The bends were soldered end to end with 25 mm long intervening pieces of copper tubing machined to the same inner diameter; for each coil 21 bends were used to give a total length of 2.677 m, i.e. 245 diameters in length. It turns out that this corresponds to a curvature ratio $\delta = 0.2$ and $z_s = l/2$ for each bend of the coil. There are several designs possible for coils with changing axis. The one chosen had the benefit of being externally similar to the constant axis coil in order to minimize the difference in outer heat transfer coefficient. Figure 7 shows the coils that were used.

The entire test section was placed in a 450 mm × 600 mm × 500 mm HDPE bath, indicated as C in Fig. 6, insulated on all sides with 19 mm thick Thermax sheathing made of glass fiber reinforced polyisocyanurate foam board with reflective aluminum foil facers. The bath was filled with distilled water heated by a 220 V, 1.4 kW Grant immersion circulator equipped with thermostatic temperature control. Two additional immersion heaters with a total capacity of 4.5 kW and equipped with thermostatic control were used for auxiliary heating to supplement the heating provided by the Grant immersion heater. A circulation pump integral with the immersion thermostat provided continuous circulation of water in the bath. As this was found to be inadequate in maintaining a spatially uniform bath temperature, dry air was bubbled through the bath at a fixed rate to provide for better mixing. Another purpose of the continuous flow and agitation of water in the bath was to achieve a high outer heat transfer coefficient in the coils. The coils were clamped to end plates placed inside the bath to provide rigidity and to minimize the effect of pump vibrations.

The in-tube inlet and exit water temperatures were measured with a pair of Teflon coated, gage 30, copper–constantan thermocouples. The junction was kept small so as to achieve accuracy in local measurements. These thermocouples were soldered to the bottom of 10 mm long pieces of 2.36 mm diameter brass tubing penetrating the tube wall of the conditioner coils close to the ends of the test coil section. The bath temperatures were monitored by three thermocouples placed at different spatial locations and depths, the

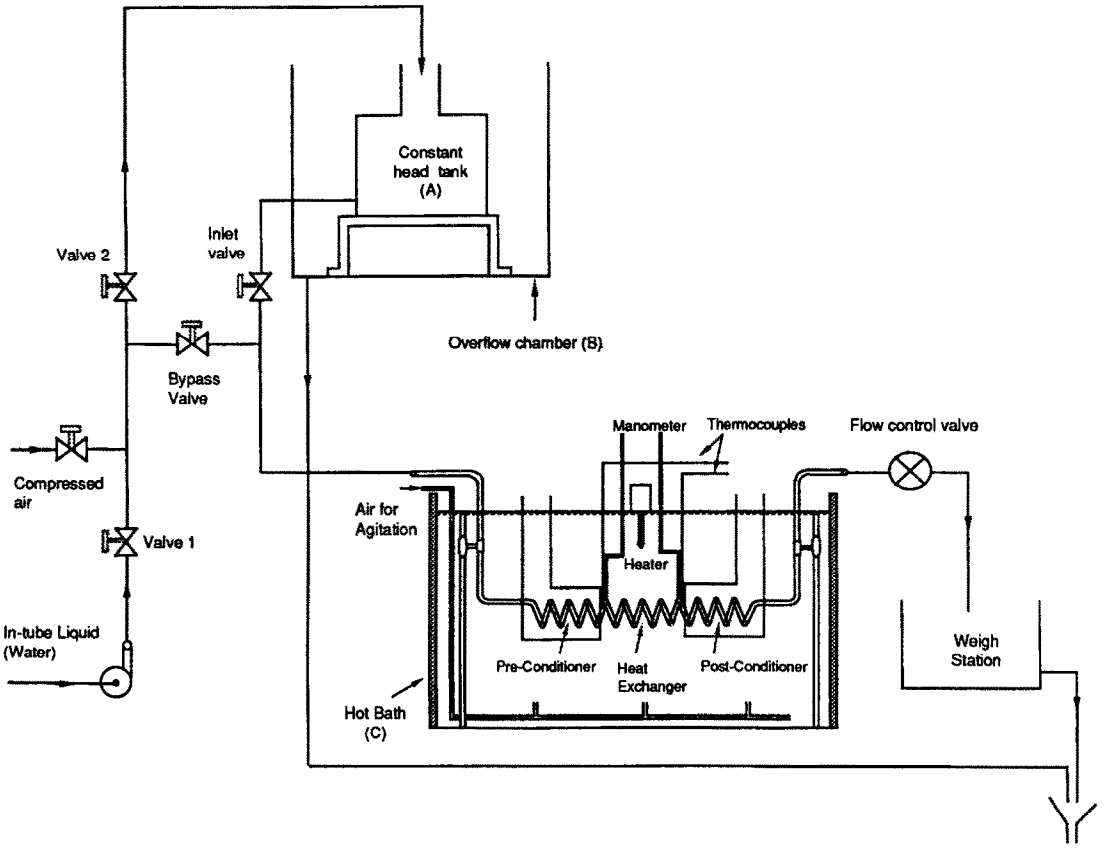

FIG. 6. Schematic of experimental set-up.

difference in temperature between them being less than 0.1°C. The flow rate was measured by timing a fixed volume of water with a Micronta stop-clock with a resolution of 0.01 s. Pressure at the inlet and exit of the test coil was measured by means of a specially fabricated manometer connected to these stations.

Since the presence of air bubbles could significantly affect the heat transfer results, it was essential to get rid of bubbles entrapped in the test and conditioning coils. This was done by using the bypass line to let water under high pressure through the coils. The bypass line was then closed and water allowed to flow directly from the overhead tank for the test. The bath was then heated to about 50°C. After steady state had been attained after several hours, the temperature, pressure and flow rates were recorded. The flow rate was then changed in steps and all readings recorded after steady state was attained.

Heat transfer coefficients

The experiments were conducted with flow of cold water in the in-tube side and warm water in the over-tube side. The total thermal resistance between the two fluids is that due to the inner and outer heat transfer coefficients, as well as the resistance of the tube wall, which is very small. Our goal is to determine the inner coefficient, which we do by measuring the overall and the outer coefficients.

Under steady state conditions, we have

$$Q = \dot{m}c\Delta T = UA_i\Delta T_{lmtd} \tag{11}$$

where Q is the rate of heat exchanged between the inner and the outer fluid, $\dot{m}$ is the mass flow rate in the tube, c is the specific heat of water, A_i is the inner heat transfer area, ΔT is the temperature change between the inlet and outlet ($=T_{in}-T_{out}$), and U is the overall heat transfer coefficient defined on the basis of the inner area. ΔT_{lmtd} is the logarithmic mean temperature difference defined by

$$\Delta T_{lmtd} = \frac{T_{in}-T_{out}}{\ln\left(\dfrac{T_{bath}-T_{in}}{T_{bath}-T_{out}}\right)}. \tag{12}$$

The inlet, outlet and bath temperatures, T_{in}, T_{out} and T_{bath} respectively, are measured for each run, in addition to $\dot{m}$. The overall heat transfer coefficient U can then be determined using fluid properties at the mean inlet–outlet temperature. The Reynolds number was determined from $\dot{m}$, using the mean velocity and the tube inner diameter as characteristic scales. The measurements were carried out over a range of flow

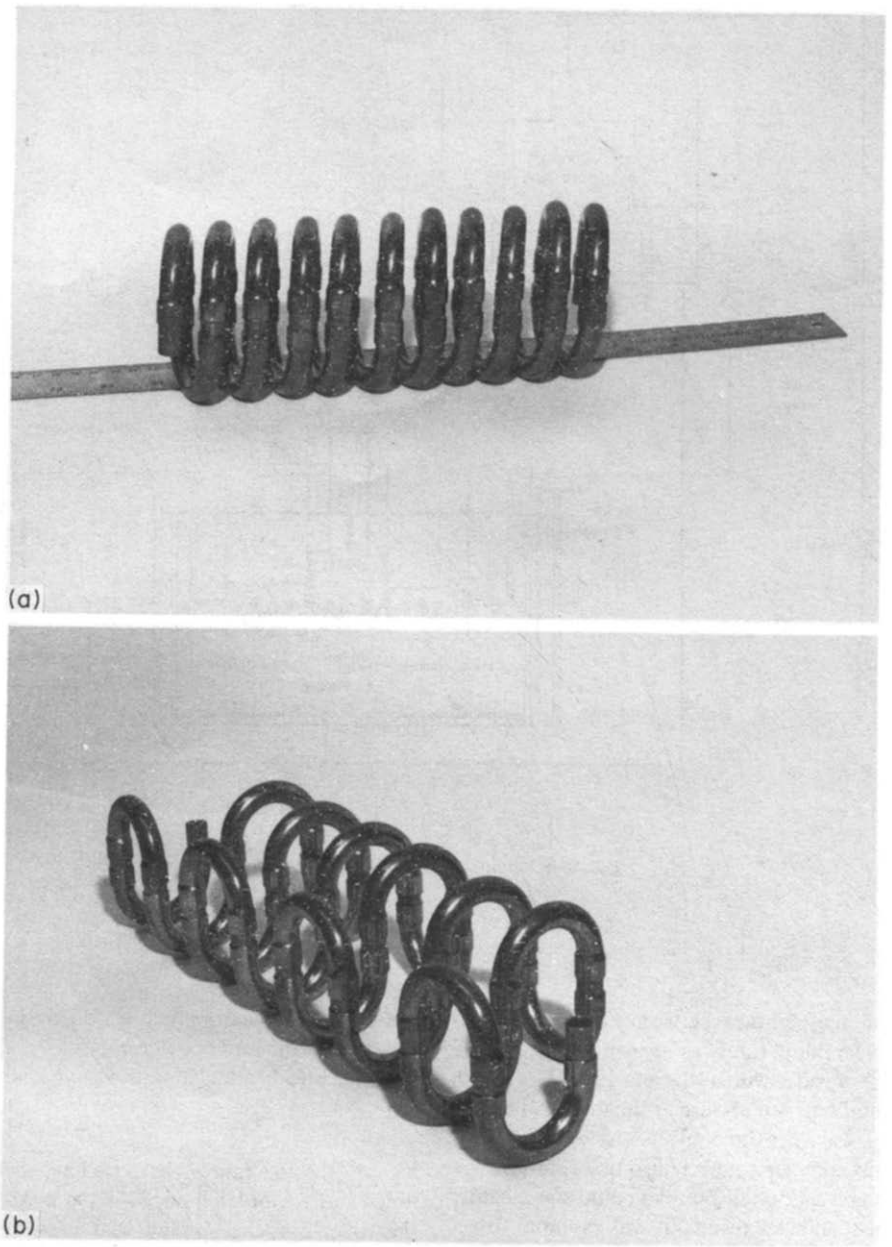

FIG. 7. Coils tested, (a) constant axis and (b) alternating axis.

Reynolds numbers, the results of which are shown in Fig. 8. The associated errors which will be discussed later are also shown. The values of U for the alternating axis configuration are seen to be consistently higher than those of the conventional constant axis configuration. The difference is larger than both the error as well as the scatter in the data.

The outer heat transfer coefficient was determined by measuring the transient response of the coils to a step change in the outside surface temperature. For this purpose, the coil was suddenly dipped in a hot water bath at a constant temperature of 50°C and the variation in wall temperature with time was obtained from a thermocouple soldered to the outer surface. The attachment of the thermocouple to the wall is critical since any thermal resistances introduced there would give a falsely lower value for the outer coefficient. After several attempts it was found most accurate to simply solder the thermocouple wire to the outer surface of the coils.

The time constant of the thermocouple, determined by plunging it into boiling water, was found to be around 0.025 s. Thus it was adequate to measure the transient response of the coils which was much slower than that. Since the conductive time scale over the coil wall thickness is two orders of magnitude smaller than this value, we are justified in assuming the coil to be a lumped mass system. The inside of the coil during

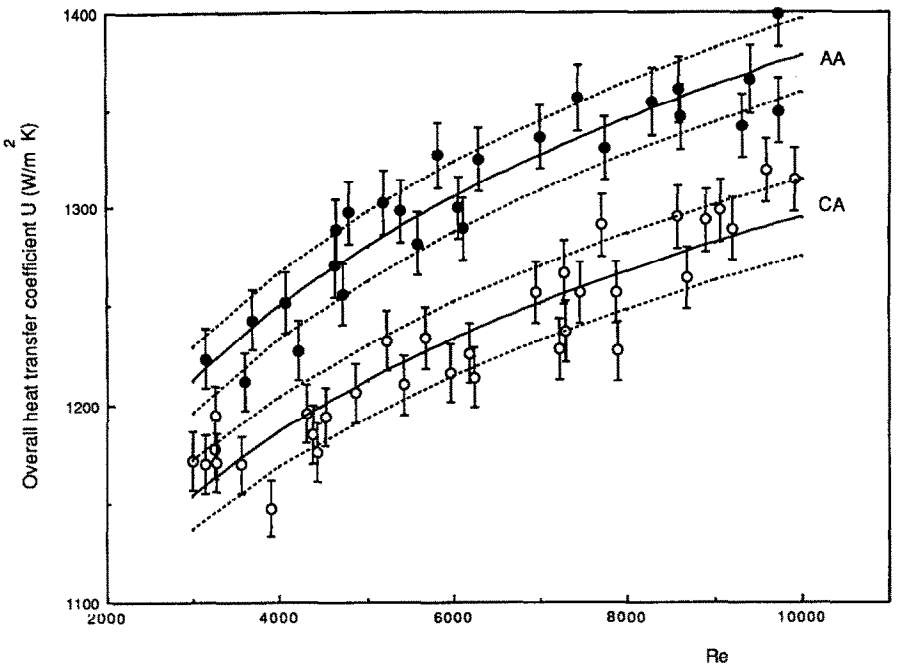

FIG. 8. Overall heat transfer coefficient.

these tests contained only air of negligible thermal capacity.

A lumped mass analysis was used to determine the outer heat transfer coefficient. The results show that $h_{o_{CA}} = 4635.4\ \mathrm{W\ m^{-2}\ K^{-1}}$ and $h_{o_{AA}} = 4809.0\ \mathrm{W\ m^{-2}\ K^{-1}}$. There is a slight difference between the h_o of the two coils because of the different geometries and flow patterns on the outside, the alternating axis coil being slightly more open to external flow.

We are, however, interested in the inner heat transfer coefficient, since it is within the tube that chaotic mixing occurs. This is obtained from

$$\frac{1}{UA_i} = \frac{1}{h_i A_i} + \frac{\ln(r_o/r_i)}{2\pi Lk} + \frac{1}{h_o A_o} \tag{13}$$

where k is the thermal conductivity of the wall, r_o and r_i are the outer and inner radii, L is the total length of the coil, h_i is the inner heat transfer coefficient. This coefficient is shown in Fig. 9. A least squares fit on the data gives

$$h_{i_{CA}} = 545.99\, Re^{0.123} \left(\frac{\mathrm{W}}{\mathrm{m^2\,K}}\right) \tag{14a}$$

$$h_{i_{AA}} = 512.04\, Re^{0.138} \left(\frac{\mathrm{W}}{\mathrm{m^2\,K}}\right). \tag{14b}$$

The enhancement factor due to the presence of chaotic mixing is then

$$\frac{h_{i_{AA}}}{h_{i_{CA}}} = 0.938\, Re^{0.015}. \tag{15}$$

This ratio is graphed in Fig. 10. The shape of this curve is qualitatively similar to that found by analysis and shown in Fig. 4.

Pressure drop measurements

The maximum flow rate and Reynolds number that could be attained were determined by the maximum height to which the overhead tank could be raised. This in our case was a Reynolds number of less than 10 000. It is important to relate this value to the critical Reynolds number for transition from laminar to turbulent flow which had to be determined by experimentation.

The onset of instability in a straight pipe is a subcritical Hopf bifurcation, with large amplitude perturbations and nonlinear phenomena being responsible for transition from laminar to turbulent flow. The friction factor for this case usually undergoes a jump as the Reynolds number is increased through the transition region. In a coiled tube, on the other hand, transition is a smooth event with the friction factor–Reynolds number curve undergoing only a change in slope at transition [27]. This instability is most likely due to a supercritical Hopf bifurcation.

Figure 11 shows the friction factor that was determined for the two coils. For this data only the Reynolds number limit was pushed higher by using a faucet as the water supply. Though the alternating axis coil has a friction factor slightly larger than the constant axis coil, a linear fit for both sets of data has been shown for the laminar and turbulent branches of the friction factor curve in a log–log plot. The intersection can be considered to give the critical Reynolds number for transition. It can be pointed out that of the two

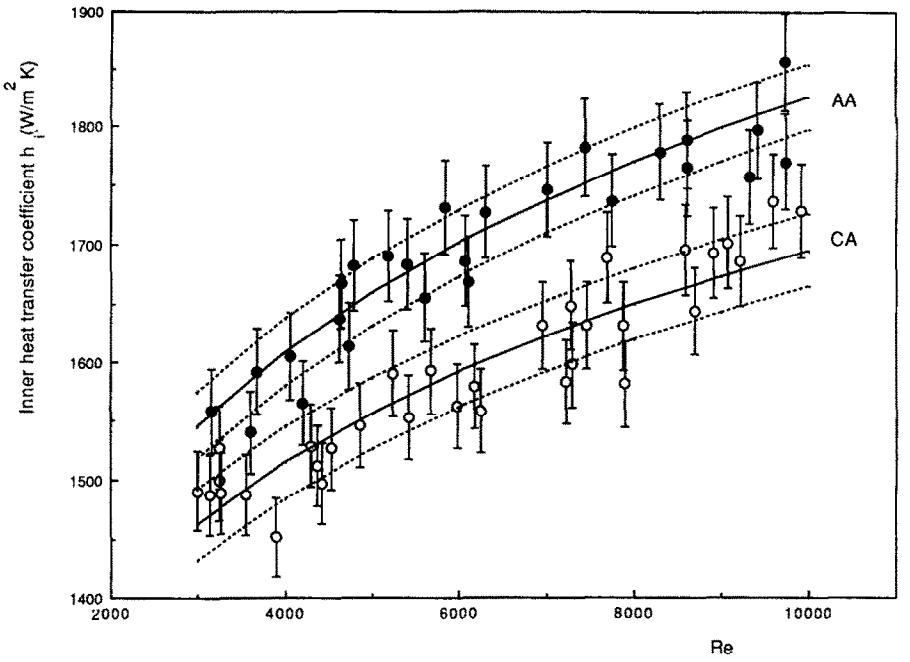

FIG. 9. Inner heat transfer coefficient as a function of Reynolds number.

the alternating axis coil shows a smoother transition. However, both coils show almost an identical critical Reynolds number of 7270 ± 70. This must be kept in mind when interpreting the results of chaotic mixing. The enhancement of heat transfer reported here is for a Reynolds number range straddling the critical value.

The relative increase in pressure drop between the two coils is calculated from the available head loss measurements. The increase shows a marginal dependence on the flow Reynolds number

$$\frac{h_{f_{AA}}}{h_{f_{CA}}} = 0.7882\, Re^{0.029}. \tag{16}$$

This is also plotted in Fig. 10 overlaying the enhancement in inside heat transfer coefficient. The increase is much smaller than that of the heat transfer coefficient.

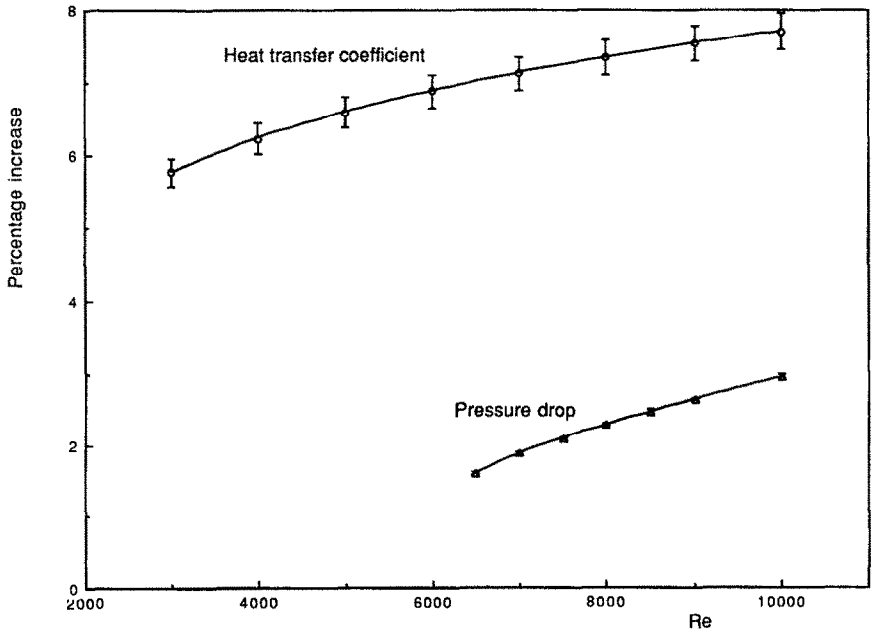

FIG. 10. Relative increase in inner heat transfer coefficient and pressure drop.

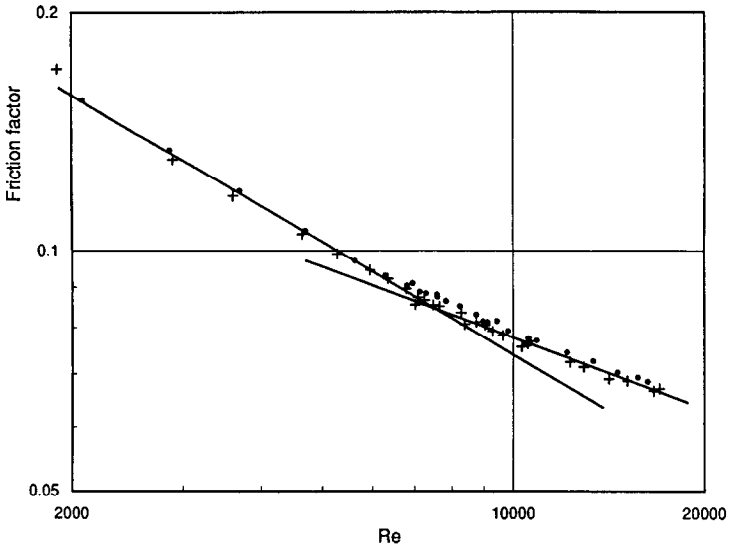

FIG. 11. Friction factor. Alternating axis *, constant axis +.

Estimation of measurement uncertainty

An attempt has been made to prescribe uncertainty estimates for the heat transfer coefficient and the pressure drop so as to enable a meaningful comparison between the two coils. Uncertainties for measured quantities are based on measurement resolution and scatter in the data while those for derived quantities are calculated using the Kline–McClintock method [28]. The overall and inner heat transfer coefficients are estimated to have uncertainties of $\pm 1.25\%$ and 2.4% respectively. The envelope of these limits over the mean, representing $\pm\sigma$ with a 68% confidence limit, is depicted in Figs. 8 and 9.

The estimated uncertainty is observed to be smaller than the difference between the two coils, so that the conclusions drawn are indeed meaningful. It is also important to note that the region defined by the $\pm\sigma$ envelope for the alternating axis coil is distinctly above that of the constant axis coil. Thus there is a small but definite difference in the inner heat transfer coefficient value for the two coils.

The uncertainty in the pressure measurements is due to errors in reading the meter scales as well as a slight unsteadiness in the water levels. It is estimated to be ± 1.5 mm within a 68% confidence limit.

CONCLUSIONS

It has been demonstrated here that periodic spatial modulation of the coil axis as in the alternating axis geometry leads to chaotic particle trajectories. Chaotic pathlines conduce not only to better mixing but also to an increased heat transfer. Numerical simulations show that the alternating axis geometry displays convective heat transfer enhancement which is more than that of constant axis coils representing conventional coiling geometry. Experiments confirm that the effect of increased mixing is also manifested as an increased heat transfer coefficient. Increased mixing also leads to larger momentum transport in the radial direction and to a higher pressure drop. The experiments show an enhancement of 6–8% in the in-tube heat transfer coefficient with a corresponding pressure drop increase of 1.5–2.5% over a Reynolds number range of 3000–10 000. Only qualitative comparisons between theory and experiment were possible since the Reynolds number in the experiments was much higher than that possible in the numerical simulations. The experiments do demonstrate the heat transfer enhancement due to chaotic mixing.

The dependence of the enhancement of heat transfer by chaotic mixing on flow and fluid parameters is now evident. The enhancement factor goes up with increasing flow Reynolds number because the secondary flow also increases. It increases with fluid Prandtl number because the higher the Prandtl number of the fluid, the more dependent is heat transfer on advection. It is also found that the increase in heat transfer enhancement due to chaotic mixing is several times the increase in the pressure drop. In other words the Reynolds analogy does not hold. This is because the nature of the flow changes completely as one goes from regular to chaotic mixing, even though the velocity field at a given section remains the same. On decreasing the fluid thermal conductivity, while keeping all other properties and flow quantities the same, the hydrodynamics is not altered and the pressure drop remains the same; however, the heat transfer does change, being larger for the case of chaotic mixing due to the flatter temperature profile.

So far the studies have been of geometries that are not calculated or optimized in any sense. Other geometries and fluids may provide larger improvements. It is also possible that chaotic mixing may be used to enhance heat transfer in other types of flows and to augment enhancement due to other mixing

techniques. Chaotic mixing is more efficient than regular mixing and can be used for all transport phenomena.

Acknowledgements—We thank the Gas Research Institute for sponsoring this research under Contract No. 5090-260-1971.

REFERENCES

1. A. Zukauskas, Heat transfer augmentation in single-phase flow, *Proc. 8th Int. Heat Transfer Conf.*, Vol. 1, pp. 47–57. Hemisphere, Washington, D.C. (1986).
2. S. V. Patankar, V. S. Pratap and D. B. Spalding, Prediction of laminar flow and heat transfer in helically coiled pipes, *J. Fluid Mech.* **62,** 539–551 (1974).
3. Y. Mori and W. Nakayama, Study on forced convective heat transfer in curved pipe (1st report, Laminar region), *Int. J. Heat Mass Transfer* **8,** 67–82 (1965).
4. C. E. Kalb and J. D. Seader, Heat and mass transfer phenomena for viscous flow in curved circular tubes, *Int. J. Heat Mass Transfer* **15,** 801–817 (1972).
5. J. M. Tarbell and M. R. Samuels, Momentum and heat transfer in helical coils, *Chem. Engng J.* **5,** 117–127 (1973).
6. M. A. Abul-Hamayel and K. J. Bell, Heat transfer in helically coiled tubes with laminar flow, 79-WA/HT-11 (1979).
7. M. Chávez, W. Zhixue and M. Sen, Turbulent convection in helicoidal tubes, *Wärme- und Stoffübertragung* **22,** 55–60 (1988).
8. R. K. Shah and S. D. Joshi, Convective heat transfer in curved ducts. In *Handbook of Single-Phase Convective Heat Transfer* (Edited by S. Kakaç, R. K. Shah and W. Aung). Wiley, New York (1987).
9. H. Aref, Stirring by chaotic advection, *J. Fluid Mech.* **143,** 1–21 (1984).
10. H. Aref, Chaotic advection in a Stokes flow, *Physics Fluids* **29,** 3515–3521 (1986).
11. J. Chaiken, R. Chevray, M. Tabor and Q. M. Tam, Experimental study of Lagrangian turbulence in a Stokes flow, *Proc. R. Soc. Lond.* **A408,** 165–174 (1986).
12. W. L. Chien, H. Rising and J. M. Ottino, Laminar mixing and chaotic mixing in several cavity flows, *J. Fluid Mech.* **170,** 355–377 (1986).
13. S. W. Jones and H. Aref, Chaotic advection in pulsed source–sink systems, *Physics Fluids* **31,** 469–485 (1988).
14. S. Ghosh, H.-C. Chang and M. Sen, Heat transfer enhancement due to slender recirculation and chaotic transport between counter-rotating eccentric cylinders, *J. Fluid Mech.* (to be published).
15. D. V. Khakhar, J. G. Franjione and J. M. Ottino, A case study of chaotic mixing in deterministic flows: the partitioned pipe mixer, *Chem. Engng Sci.* **42,** 2909–2926 (1987).
16. C. S. Lee, J. J. Ou and S. H. Chen, Quantification of mixing from the Eulerian perspective: flow through a curved tube, *Chem. Engng Sci.* **42,** 2484–2486 (1987).
17. S. W. Jones, O. M. Thomas and H. Aref, Chaotic advection by laminar flow in a twisted pipe, *J. Fluid Mech.* **209,** 335–357 (1989).
18. Y. Le Guer and H. Peerhossaini, Order breaking in Dean flow, *Physics Fluids A* **3,** 1029–1032 (1991).
19. H. Peerhossaini and Y. Le Guer, Chaotic motion in the Dean instability flow—a heat exchanger design, *Bull. APS* **35,** 2229 (1990).
20. A. K. Saxena and K. D. P. Nigam, Coiled configuration for flow inversion and its effect on residence time distribution, *A.I.Ch.E. Jl* **30,** 363–368 (1984).
21. S. A. Berger, L. Talbot and L. S. Yao, Flow in curved ducts, *Ann. Rev. Fluid Mech.* **15,** 461–512 (1983).
22. W. R. Dean, Note on the motion of fluid in a curved pipe, *Phil. Mag. J. Sci.* **4** (7th series), 208–223 (1927).
23. W. R. Dean, The stream-line motion of fluid in a curved pipe, *Phil. Mag. J. Sci.* **5,** 673–695 (1928).
24. A. Wolf, B. Swift, L. Swinnery and A. Vastano, Determining Lyapunov exponents from a time series, *Physica D* **16,** 285–317 (1985).
25. L. A. M. Janssen and C. J. Hoogendoorn, Laminar convective heat transfer in helical coiled tubes, *Int. J. Heat Mass Transfer* **21,** 1197–1206 (1978).
26. A. N. Dravid, K. A. Smith, E. W. Merrill and P. L. T. Brain, Effect of secondary fluid motion on laminar flow in helically coiled tubes, *A.I.Ch.E. Jl* **17,** 1114–1122 (1971).
27. H. Ito, Friction factors for turbulent flow in curved pipes, *ASME J. Basic Engng* **81,** 123–134 (1959).
28. S. J. Kline and F. A. McClintock, Describing uncertainties in single sample experiments, *Mech. Engng* **75,** 3–8 (1953).

AMELIORATION DU TRANSFERT THERMIQUE PAR MELANGE CHAOTIQUE DANS DES TUBES HELICOIDAUX

Résumé—On examine le mélange chaotique comme moyen pour augmenter la convection thermique dans un tube hélicoïdal. Il est montré que des modifications simples de la géométrie de l'hélice peuvent être avantageuses. L'étude est focalisée sur une géométrie avec l'axe de la bobine tourné de 90° d'une façon périodique et des comparaisons sont faites avec une bobine ordinaire. Des parcours de particules sont calculés en utilisant la solution classique de perturbation de Dean pour l'écoulement secondaire. Le mélange chaotique est confirmé par un exposant positif de Lyapunov. Le champ de température calculé numériquement montre que le mélange chaotique est responsable d'un aplatissement considérable du profil de température et d'un accroissement du transfert thermique convectif. Des expériences sont conduites avec l'eau sur deux géométries de tubes enroulés, pour un domaine de nombre de Reynolds entre 3000 et 10 000. Les enroulements sont identiques sauf que l'un est conventionnel avec axe unique et que l'autre à un axe alterné. Ce dernier montre un coefficient de convection supérieur de 6–8% dû au mélange chaotique, avec une perte de pression accrue de 1,5–2,5%.

VERBESSERUNG DES WÄRMEÜBERGANGS IN ROHRWENDELN DURCH CHAOTISCHES MISCHEN

Zusammenfassung—In der vorliegenden Arbeit wird die Verbesserung des konvektiven Wärmeübergangs innerhalb von Rohrwendeln infolge chaotischen Mischens untersucht. Es wird gezeigt, daß einfache Veränderungen der Wendelgeometrie vorgenommen werden können um den genannten Effekt auszunutzen. Die Untersuchung beschäftigt sich mit einer Wendelgeometrie, bei der die Wendelachse periodisch um jeweils 90° gedreht wird. Zum Vergleich werden auch Versuche mit einer Rohrwendel ohne diese Verformung durchgeführt. Partikeltrajektorien in der Strömung werden mit der klassischen Perturbationslösung für die Sekundärströmung nach Dean bestimmt. Das Vorliegen von chaotischer Vermischung wird durch das Auftreten positiver Lyapunov-Koeffizienten bestätigt. Das Temperaturfeld wird numerisch berechnet, wobei sich zeigt, daß das Temperaturprofil durch chaotische Vermischung deutlich abgeflacht wird und der konvektive Wärmeübergang sich verbessert. Es werden Experimente mit Wasser in zwei Rohrwendelgeometrien bei Reynolds-Zahlen zwischen 3000 und 10 000 durchgeführt. Die beiden untersuchten Wendelgeometrien sind identisch bis auf die Anordnung der Wendelachse—die eine ist konventionell konstant, während die andere alterniert. Letztere zeigt ein um 6–8% höheren Wärmeübergangskoeffizienten auf der Rohrinnenseite infolge der chaotischen Vermischung, während der Druckverlust lediglich um 1,5–2,5% zunimmt.

ИНТЕНСИФИКАЦИЯ ТЕПЛОПЕРЕНОСА В ВИТЫХ ТРУБАХ ЗА СЧЕТ ХАОТИЧЕСКОГО ПЕРЕМЕШИВАНИЯ

Аннотация—Исследуется хаотическое перемешивание как способ интенсификации конвективного теплопереноса в змеевиках. Показано, что рассматриваемое явление может использоваться в простых модификациях геометрии спиралей. Основное внимание уделяется геометрии, в которой ось спирали периодически поворачивается на 90°, и проводятся сравнения со спиралью без поворота оси. Пути частиц рассчитываются для возмущений вторичного течения. Наличие хаотического перемешивания подтверждается положительным знажением показателя Ляпунова. Численные расчеты теплового поля показывают, что хаотическое перемешивание вызывает существенное сглаживание температурного профиля и увеличение конвективного теплопереноса. Эксперименты проводятся с использованием воды на геометриях двух витых труб в широком диапазоне изменения числа Рейнольдса, составляющего 3000–10 000. Спирали илентичны во всех отношениях за исключением того, что одна из них является обычной с постоянной осью, а другая—с переменной осью. Коэффициент теплопереноса в последнем случае на 6–8% выше за счет хаотического перемешивания, и соответствующий перенад давления больше на 1,5–2,5%.